
Goal-directed Generation of Discrete Structures with Conditional Generative Models

Amina Mollaysa

University of Geneva
University of Applied Sciences Western Switzerland
maolaaisha.aminanmu@hesge.ch

Brooks Paige

University College London
Alan Turing Institute
b.paige@ucl.ac.uk

Alexandros Kalousis

University of Geneva
University of Applied Sciences Western Switzerland
alexandros.kalousis@hesge.ch

Abstract

Despite recent advances, goal-directed generation of structured discrete data remains challenging. For problems such as program synthesis (generating source code) and materials design (generating molecules), finding examples which satisfy desired constraints or exhibit desired properties is difficult. In practice, expensive heuristic search or reinforcement learning algorithms are often employed. In this paper we investigate the use of conditional generative models which directly attack this inverse problem, by modeling the distribution of discrete structures given properties of interest. Unfortunately, maximum likelihood training of such models often fails with the samples from the generative model inadequately respecting the input properties. To address this, we introduce a novel approach to directly optimize a reinforcement learning objective, maximizing an expected reward. We avoid high-variance score-function estimators that would otherwise be required by sampling from an approximation to the normalized rewards, allowing simple Monte Carlo estimation of model gradients. We test our methodology on two tasks: generating molecules with user-defined properties, and identifying short python expressions which evaluate to a given target value. In both cases we find improvements over maximum likelihood estimation and other baselines.

1 Introduction

Machine learning models for structured data such as program source code and molecules typically represent the data as a sequence of discrete values. However, even as recent advances in sequence models have made great strides in predicting properties from the sequences, the inverse problem of generating sequences for a given set of pre-defined properties remains challenging. These sorts of structure design problems have great potential in many application areas; e.g., in materials design, where one may be interested in generating molecular structures appropriate as batteries, photovoltaics, or drug targets. However, as the underlying sequence is discrete, directly optimizing it with respect to target properties becomes problematic: gradients are unavailable, meaning we can not directly estimate the change in (say) a material that would correspond to a desired change in properties.

An open question is how well machine learning models can help us quickly and easily explore the space of discrete structures that correspond to particular properties. There are a few approaches based on generative models which aim to directly simulate likely candidates. Neural sequence models [23, 2] are used to directly learn the conditional distributions by maximizing conditional log likelihoods and have shown potential in text generation, image captioning and machine translation.

Fundamentally, a maximum likelihood (ML) objective is a poor choice if our main goal is not learning the exact conditional distribution over the data, but rather to produce a diverse set of generations which match a target property. Reinforcement learning (RL) offers an alternative, explicitly aiming to maximize an expected reward. The fundamental difference is between “many to one” and “one to many” settings. A ML objective works well for prediction tasks where the goal is to match each input to its exact output. For instance, consider the models which predict properties from molecules, since each molecule has a well-determined property. However, for the inverse problem the data severely underspecifies the mapping, since any given property combination has many diverse molecules which match; nearly all of these are not present in the training data. As the ML objective is only measured on the training pairs, any output that is different from the training data target is penalized. Therefore, a model which generates novel molecules with the correct properties would be penalized by ML training, as it does not produce the exact training pairs; but, it would have a high reward and thus be encouraged by an RL objective.

Recent work has successfully applied policy gradient optimization [25] on goal oriented sequence generation tasks [6, 11]. These methods can deal with the non-differentiability of both the data and the reward function. However, policy gradient optimization becomes problematic especially in high dimensional action spaces, requiring complicated additional variance reduction techniques [10]. Those two schemes, ML estimation and RL training, are both equivalents to minimizing a KL divergence between an exponentiated reward distribution (defined accordingly) and model distribution but in the opposite directions [18]. If all we care about is generating realistic samples, the direction corresponding to the RL objective is the more appropriate to optimize [13]: the only question is how to make training efficient.

We formulate the conditional generation of discrete sequence as a reinforcement learning objective to encourage the generation of sequences with specific desired properties. To avoid the inefficiency of the policy gradient optimization, which requires large sample sizes and variance reduction techniques, we propose an easy alternative formulation that instead leverages the underlying similarity structure of a training dataset.

2 Methods

In this section, we introduce a new approach which targets an RL objective, maximizing expected reward, to directly learn conditional generative models of sequences given target properties. We sidestep the high variance of the gradient estimation which would arise if we directly apply policy gradient methods, by an alternative approximation to the expected reward that removes the need to sample from the model itself.

Suppose we are given a training set of pairs $\mathcal{D} = \{(\mathbf{x}_i, \mathbf{y}_i)\}, i = 1, \dots, N$, where $\mathbf{x}_i = x_{i,1..T}$ is a length T sequence of discrete variables, and $\mathbf{y}_i \in \mathcal{Y}$ is the corresponding output vector, whose domain may include discrete and continuous dimensions. Assume the input-output instances $(\mathbf{x}_i, \mathbf{y}_i)$ are i.i.d. sampled from some unknown probability distribution $\tilde{p}(\mathbf{x}, \mathbf{y})$, with f the ground truth function that maps \mathbf{x}_i to \mathbf{y}_i for all pairs $(\mathbf{x}_i, \mathbf{y}_i) \sim \tilde{p}(\mathbf{x}, \mathbf{y})$. Our goal is to learn a distribution $p_\theta(\mathbf{x}|\mathbf{y})$ such that for a given \mathbf{y} in $\tilde{p}(\mathbf{y})$, we can generate samples \mathbf{x} that have properties close to \mathbf{y} .

2.1 Maximizing expected reward

We can formulate this learning problem in a reinforcement learning setting, where the model we want to learn resembles learning a stochastic policy $p_\theta(\mathbf{x}|\mathbf{y})$ that defines a distribution over \mathbf{x} for a given state \mathbf{y} . For each \mathbf{x} that is generated for a given state \mathbf{y} , we can define a reward function $R(\mathbf{x}; \mathbf{y})$ such that it assigns higher value for \mathbf{x} when $d(f(\mathbf{x}), \mathbf{y})$ is small and vice versa, where d is a meaningful distance defined on \mathcal{Y} . This model can be learned by maximizing the expected reward

$$\mathcal{J} = \mathbb{E}_{\tilde{p}(\mathbf{y})} \mathbb{E}_{p_\theta(\mathbf{x}|\mathbf{y})} [R(\mathbf{x}; \mathbf{y})]. \quad (1)$$

When there is a natural notion of distance $d(\mathbf{y}, \mathbf{y}')$ for values in \mathcal{Y} , then we can define a reward $R(\mathbf{x}; \mathbf{y}) = \exp\{-\lambda d(f(\mathbf{x}), \mathbf{y})\}$. If the model $p_\theta(\mathbf{x}|\mathbf{y})$ defines a distribution over discrete random variables or if the reward function is non-differentiable, a direct approach requires admitting high-variance score-function estimators of the gradient of the form

$$\nabla_\theta \mathcal{J} = \mathbb{E}_{\tilde{p}(\mathbf{y})} \mathbb{E}_{p_\theta(\mathbf{x}|\mathbf{y})} [R(\mathbf{x}; \mathbf{y}) \nabla_\theta \log p_\theta(\mathbf{x}|\mathbf{y})]. \quad (2)$$

The inner expectation in this gradient estimator would typically be Monte Carlo approximated via sampling from the model $p_\theta(\mathbf{x}|\mathbf{y})$. The reward is often sparse in high dimensional action spaces,

leading to a noisy gradient estimate. Typically, to make optimization work with score-function gradient estimators, we need large samples sizes, control variate schemes, or even warm-starting from pre-trained models. Instead of sampling from the model distribution and look for the direction where we get high rewards, we consider an alternative breakdown of the objective to avoid direct Monte Carlo simulation from $p_\theta(\mathbf{x}|\mathbf{y})$.

Assume we have a finite non-negative reward function $R(\mathbf{x}; \mathbf{y})$, with $0 \leq R(\mathbf{x}; \mathbf{y}) < \infty$, and let $c(\mathbf{y}) = \sum_{\mathbf{x}} R(\mathbf{x}; \mathbf{y})$. We can then rewrite the objective in Eq. (1), using the observation that

$$\mathbb{E}_{p_\theta(\mathbf{x}|\mathbf{y})}[R(\mathbf{x}; \mathbf{y})] = c(\mathbf{y})\mathbb{E}_{\bar{R}(\mathbf{x}|\mathbf{y})}[p_\theta(\mathbf{x}|\mathbf{y})], \quad (3)$$

where we take the expectation instead over the ‘‘normalized’’ rewards distribution $\bar{R}(\mathbf{x}|\mathbf{y}) = R(\mathbf{x}; \mathbf{y})/c(\mathbf{y})$. (A detailed derivation is in Appendix A.) Leaving aside for the moment any practical challenges of normalizing the rewards, we note that this formulation allows us instead to employ a path-wise derivative estimator [21]. Using the data distribution to approximate expectations over $\tilde{p}(\mathbf{y})$ in Eq. 2, we have

$$\nabla_\theta \mathcal{J} \approx \frac{1}{N} \sum_{i=1}^N c(\mathbf{y}_i) \mathbb{E}_{\bar{R}(\mathbf{x}|\mathbf{y}_i)}[\nabla_\theta p_\theta(\mathbf{x}|\mathbf{y}_i)]. \quad (4)$$

To avoid numeric instability as $p_\theta(\mathbf{x}|\mathbf{y})$ may take very small values, we instead work in terms of log probabilities. This requires first noting that $\arg \max_\theta \mathcal{J} = \arg \max_\theta \log \mathcal{J}$ where we then have:

$$\begin{aligned} \log \mathcal{J} &= \log (\mathbb{E}_{\tilde{p}(\mathbf{y})} c(\mathbf{y}) \mathbb{E}_{\bar{R}(\mathbf{x}|\mathbf{y})} [p_\theta(\mathbf{x}|\mathbf{y})]) \geq \mathbb{E}_{\tilde{p}(\mathbf{y})} \log (c(\mathbf{y}) \mathbb{E}_{\bar{R}(\mathbf{x}|\mathbf{y})} [p_\theta(\mathbf{x}|\mathbf{y})]) \\ &= \mathbb{E}_{\tilde{p}(\mathbf{y})} \log \mathbb{E}_{\bar{R}(\mathbf{x}|\mathbf{y})} [p_\theta(\mathbf{x}|\mathbf{y})] + \text{const.} \end{aligned}$$

From Jensen’s inequality, we have $\log \mathbb{E}_{\bar{R}(\mathbf{x}|\mathbf{y})} [p_\theta(\mathbf{x}|\mathbf{y})] \geq \mathbb{E}_{\bar{R}(\mathbf{x}|\mathbf{y})} [\log p_\theta(\mathbf{x}|\mathbf{y})]$, which motivates optimizing instead a lower-bound on $\log \mathcal{J}$, an objective we refer to as

$$\mathcal{L} = \mathbb{E}_{\tilde{p}(\mathbf{y})} \mathbb{E}_{\bar{R}(\mathbf{x}|\mathbf{y})} [\log p_\theta(\mathbf{x}|\mathbf{y})] \quad (5)$$

Again using the data distribution to approximate expectations over $\tilde{p}(\mathbf{y})$, the gradient is simply

$$\nabla_\theta \mathcal{L} \approx \frac{1}{N} \sum_{i=1}^N \mathbb{E}_{\bar{R}(\mathbf{x}|\mathbf{y}_i)} [\nabla_\theta \log p_\theta(\mathbf{x}|\mathbf{y}_i)]. \quad (6)$$

2.2 Approximating expectations under the normalized reward distribution

Of course, in doing this we have introduced the potentially difficult task of sampling directly from the normalized reward distribution. Fortunately, if we are provided with a reasonable training dataset \mathcal{D} which well represents $\tilde{p}(\mathbf{x}, \mathbf{y})$ then we propose not sampling new values at all, but instead re-weighting examples \mathbf{x} from the dataset as appropriate to approximate the expectation with respect to the normalized reward.

For a fixed reward function $R(\mathbf{x}, \mathbf{y}) = \exp\{-\lambda d(f(\mathbf{x}), \mathbf{y})\}$, when restricting to the training set we can instead re-express the normalized reward distribution in terms of a distribution over training indices. Given a fixed \mathbf{y}_i , consider the rewards as restricted to values $\mathbf{x} \in \{\mathbf{x}_1, \dots, \mathbf{x}_N\}$; each potential \mathbf{x}_j has a paired value $\mathbf{y}_j = f(\mathbf{x}_j)$. Using our existing dataset to approximate the expectations in our objective, we have for each \mathbf{y}_i

$$\mathbb{E}_{\bar{R}(\mathbf{x}|\mathbf{y}_i)} [\log p_\theta(\mathbf{x}|\mathbf{y}_i)] \approx \sum_{j=1}^N \bar{R}(\mathbf{x}_j|\mathbf{y}_i) \log p_\theta(\mathbf{x}_j|\mathbf{y}_i) \approx \mathbb{E}_{p(j|i)} [\log p_\theta(\mathbf{x}_j|\mathbf{y}_i)] \quad (7)$$

where the distribution over indices $p(j|i)$ is defined as

$$p(j|i) = \frac{R(\mathbf{x}_j; \mathbf{y}_i)}{\sum_{j=1}^N R(\mathbf{x}_j; \mathbf{y}_i)}. \quad (8)$$

Note that there are two normalized distributions which we consider. The first $\bar{R}(\mathbf{x}|\mathbf{y}_i)$ is defined by normalizing the reward across the entire space of possible values \mathbf{x} ,

$$\bar{R}(\mathbf{x}|\mathbf{y}_i) = \frac{R(\mathbf{x}; \mathbf{y}_i)}{\sum_{\mathbf{x}} R(\mathbf{x}; \mathbf{y}_i)} = \frac{R(\mathbf{x}; \mathbf{y}_i)}{c(\mathbf{y}_i)} \quad (9)$$

The second is $p(j|i)$ which is defined by normalizing instead across the empirical distribution of values \mathbf{x} in the training set, yielding the distribution over indices as given in equation 8. The restriction of $\bar{R}(\mathbf{x}|\mathbf{y}_i)$ to the discrete points in the training set is not the same and our approximation is off by a scalar multiplicative factor $\sum_{j=1}^N R(\mathbf{x}_j|\mathbf{y}_i) / \sum_{\mathbf{x}} R(\mathbf{x}|\mathbf{y}_i)$. However, this factor does not dramatically affect outcomes: its value is *independent of* \mathbf{x} , depending only on \mathbf{y}_i . Any bias which is introduced would come into play only in the evaluation of Eq. (6), where entries from different \mathbf{y} values may effectively be assigned different weights. So while this may affect unconditional generations from the model, and means that some \mathbf{y} values may be inappropriately considered “more important” than others during training, it should not directly bias *conditional* generation for a fixed \mathbf{y} . Full discussion of this point is in Appendix B.

Thus, for any choice of reward, we can define a sampling distribution from which to propose examples \mathbf{x}_j given \mathbf{y}_i by computing and normalizing the rewards across (i, j) pairs in the dataset. While naively computing this sampling distribution for every i requires constructing an $N \times N$ matrix, in practice typically very few of the N datapoints have normalized rewards which are numerically much greater than zero, allowing easy pre-computation of a N array of dimension K_i where K is the maximum number of non-zero elements each entry i , under the distance $d(f(\mathbf{x}_j), \mathbf{y}_i)$. This can then later be used as a sampling distribution for \mathbf{x}_j at training time.

2.3 Sequence diversification

Our sampling procedure operates exclusively over the training instances. This, coupled with the fact that we operate over sequences of discrete elements, can restrict in a considerable manner the generation abilities of our model. To encourage a more diverse exploration of the sequence space and thus more diverse generations we couple our objective with an entropy regulariser. In addition to the likelihood of the generated sequences, we propose also maximizing their entropy, with

$$\max_{\theta} \sum_{i=1}^N [\mathbb{E}_{\bar{R}(\mathbf{x}|\mathbf{y}_i)} [\log p_{\theta}(\mathbf{x}|\mathbf{y}_i)] + \lambda H(p_{\theta}(\mathbf{x}|\mathbf{y}_i))]. \quad (10)$$

In a discrete sequence model the gradient of the entropy term can be computed as

$$\nabla_{\theta} H(p_{\theta}(\mathbf{x}|\mathbf{y})) = -\nabla_{\theta} \mathbb{E}_{p_{\theta}(\mathbf{x}|\mathbf{y})} \log p_{\theta}(\mathbf{x}|\mathbf{y}) = -\mathbb{E}_{p_{\theta}(\mathbf{x}|\mathbf{y})} [(1 + \log p_{\theta}(\mathbf{x}|\mathbf{y})) \nabla_{\theta} \log p_{\theta}(\mathbf{x}|\mathbf{y})]; \quad (11)$$

for details see Appendix C. Suffice it to say, a naïve Monte Carlo approximation suffers from high variance and sample inefficiency. We instead use an easily-differentiable approximation to the entropy. We decompose the entropy of the generated sequence into a sequence of individual entropy terms

$$H(p_{\theta}(\mathbf{x}|\mathbf{y})) = -\mathbb{E}_{p_{\theta}(\mathbf{x}|\mathbf{y})} \sum_{t=1}^T \log p_{\theta}(\mathbf{x}_t|\mathbf{x}_{1:t-1}, \mathbf{y}) = H(p_{\theta}(\mathbf{x}_1|\mathbf{y})) + \sum_{t=2}^T E_{p_{\theta}(\mathbf{x}_{1:t-1}|\mathbf{y})} [H(p_{\theta}(\mathbf{x}_t|\mathbf{x}_{1:t-1}, \mathbf{y}))].$$

We can compute analytically the entropy of each individual $p_{\theta}(\mathbf{x}_t|\mathbf{x}_{1:t-1}, \mathbf{y})$ term, since this is a discrete probability distribution with a small number of possible outcomes given by the dictionary size, and use sampling to generate the values we condition on at each step. Instead of using a Monte Carlo estimation of the expectation term, we generate the sequence in a greedy manner, selecting the maximum probability element, \mathbf{x}_t^* , at each step. This results in approximating the entropy term as

$$H(p_{\theta}(\mathbf{x}|\mathbf{y})) \approx H[p_{\theta}(\mathbf{x}_1|\mathbf{y})] + \sum_{t=2}^T [H[p_{\theta}(\mathbf{x}_t|\mathbf{x}_{1:t-1}^*, \mathbf{y})]].$$

Its gradient is straightforward to compute since each individual entropy term can be computed analytically. In Appendix J we provide an experimental evaluation suggesting the above approximation outperforms simple Monte Carlo based estimates, as well as the straight-through estimator.

3 Experiments

We evaluate our training procedure on two conditional discrete structure generation tasks: generating python integer expressions that evaluate to a given value, and generating molecules which should exhibit a given set of properties. We do a complete study of our model without the use of the entropy-based regulariser and then explore the behavior of the regulariser.

```

S -> Expr Op Expr [1.0]
Expr -> Number [0.4] | Expr Op Expr [0.4] |
      L Expr Op Expr R [0.2]
Number -> Nonzero Digits [0.9] | Nonzero [0.1]
Nonzero -> 1 [0.1111] | 2 [0.1111] | 3 [0.1111] |
          4 [0.1111] | 5 [0.1111] | 6 [0.1111] |
          7 [0.1111] | 8 [0.1111] | 9 [0.1111] |
Digits -> Digit [0.95] | Digit Digits [0.05]
Digit -> 0 [0.1] | Nonzero [0.9]
Op -> '+' [0.3] | '-' [0.3] |
      '*' [0.2] | '/' [0.2]
L -> '(' [1.0]
R -> ')' [1.0]

```

Listing 1: CFG for inverse calculator

Objective	Valid	Unique	Novel
ML	0.9888 ± 0.0002	0.9681 ± 0.0004	0.9301 ± 0.0003
Ours	0.9903 ± 0.0003	0.9635 ± 0.0006	0.9271 ± 0.0005

Table 1: Python integer expression generation results

	MAE	Accuracy	Within ± 3	$-\log p(\mathbf{x} \mathbf{y})$
ML	13.917 ± 0.117	0.166 ± 0.001	0.596 ± 0.001	1.830
Ours	11.823 ± 0.145	0.166 ± 0.001	0.682 ± 0.001	1.986

Table 2: Python integer expression *conditional* generation results

In all experiments, we model the conditional distributions $p_\theta(\mathbf{x}|\mathbf{y})$ using a 3-layer stacked LSTM sequence model; for architecture details see Appendix D and Fig. D.3. We evaluate the performance of our model both in terms of the quality of the generations, as well as its sensitivity to values of the conditioning variable \mathbf{y} . Generation quality is measured by the percentage of valid, unique, and novel sequences that the model produces, while the quality of the conditional generations is evaluated by computing the error between the value \mathbf{y} we condition on, and the property value $f(\mathbf{x})$ that the generated sequence \mathbf{x} exhibits. We compared our model against a vanilla maximum likelihood (ML) trained model, where we learn the distribution $p_\theta(\mathbf{x}|\mathbf{y})$ by maximizing the conditional log-likelihood of the training set. We also test against two additional data augmentation baselines, including the reward augmented maximum likelihood (RAML) procedure of Norouzi et al. [18].

3.1 Conditional generation of mathematical expressions

Before considering the molecule generation task, we first look at a simpler constrained “inverse calculator” problem, in which we attempt to generate python integer expressions that evaluate to a certain target value. We generate synthetic training data by sampling from the probabilistic context free grammar presented in Listing 1. We generate approximately 300k unique, valid expressions of length 30 characters or less, that evaluate to integers in the range $(-1000, 1000)$; we split them into training, test, and validation subsets. Full generation details are in Appendix E.

We define a task-specific reward based on permitting a small squared-error difference between the equations’ values and the conditioning value; i.e. $R(\mathbf{x}|y) = \exp\{-\frac{1}{2}(f(\mathbf{x}) - y)^2\}$, which means for a given candidate y_i the normalized rewards distribution forms a discretized normal distribution. We can sample appropriate matching expressions \mathbf{x}_j by first sampling a target value from y' from a Gaussian $\mathcal{N}(y'|y_i)$ truncated to $(-999, 999)$, rounding the sampled y' , and then uniformly sampling \mathbf{x} from all training examples such that $\text{EVAL}(\mathbf{x}) = \text{round}(y')$. We found training to be most stable by pre-sampling these, drawing 10 values of \mathbf{x} for each y_i in the training and validation sets and storing these as a single, larger training and validation set which can be used to directly estimate the expected reward.

To evaluate the performance of the generated integer expressions, we sample 25 expressions for 10k values in the test set; we repeat this process 6 times and report means and standard deviations. Generated expressions which evaluate to non-finite values, or to values outside the $(-1000, 1000)$ range, are discarded as invalid. In Table 1 we show the statistics for the validity, uniqueness, and novelty (relative to the training set) of the generated expressions. Both models perform well, and quite comparably; about 99% of generated expressions are valid, with few duplicates either of the other samples or of the training expressions. Table 2 reports (for the valid expressions) the mean absolute error (MAE), the exact accuracy (i.e. whether $\text{EVAL}(\mathbf{x}) = y$), an “approximate” accuracy checking if the value is within ± 3 , as well as the negative log likelihood on the test set. While the exact accuracy does not change, we do see better performance in our training regime at both MAE and approximate accuracy, suggesting that “wrong” expressions are in some sense less wrong. We also note the tradeoff between objectives: our model trained to improve generation accuracy slightly underfits in terms of test log likelihood.

3.2 Conditional generation of molecules

We now attempt to learn a model that can directly generate molecules that exhibit a given set of properties. We experiment with two datasets: QM9 [19] which contains 133k organic compounds that have up to nine heavy atoms and ChEMBL [17] of molecules that have been synthesized and tested against biological targets, which includes relatively larger molecules (up to 16 heavy atoms). For details of the datasets see Appendix D. We represent molecules by SMILES strings [24], and

Model	QM9			ChEMBL		
	Valid	Unique	Novel	Valid	Unique	Novel
ML	0.962	0.967	0.366	0.895	0.999	0.990
Ours	0.989	0.963	0.261	0.945	0.9986	0.981

Table 3: Molecule generation quality

Model	QM9		
	Validity	Unicity	Novelty
Classic data augmentation	0.937	0.980	0.464
RAML-like data augmentation	0.940	0.986	0.747
Ours + Entropy regularizer ($\lambda = 0.0008$)	0.977	0.961	0.274

Table 4: Molecule generation quality

Model	rotatable bonds	aromatic rings	QM9: MSE						
			logP	QED	TPSA	bertz	mol weight	fluorine count	# rings
ML	0.0468	0.0014	0.0390	0.0010	11.18	80.77	4.425	0.0023	0.0484
Ours	0.0166	0.0005	0.0184	0.0004	3.859	63.67	1.184	0.0004	0.0120
QM9: Correlation coefficient									
ML	0.9809	0.9944	0.9805	0.9063	0.9871	0.9843	0.9651	0.9783	0.9817
Ours	0.9937	0.9972	0.9901	0.9634	0.9954	0.9840	0.9887	1.0000	0.9948
ChEMBL: MSE									
ML	0.1552	0.0388	0.1450	0.0050	27.64	1708.	103.9	0.0128	0.0226
Ours	0.1555	0.0268	0.1320	0.0046	35.05	2512.	174.9	0.0074	0.0191
ChEMBL: Correlation coefficient									
ML	0.9936	0.9862	0.9777	0.9450	0.9906	0.9934	0.9956	0.9940	0.9931
Ours	0.9934	0.9901	0.9796	0.9496	0.9878	0.9902	0.9926	0.9966	0.9943

Table 5: Conditional generation performance for the molecules datasets.

condition on nine molecule properties which are present in the goal-directed generation tasks of Brown et al. [5]: number of rotatable bonds, number of aromatic rings, logP, QED score, tpsa, bertz, molecule weight, atom counter and number of rings; these properties can all be readily estimated by open-source cheminformatics software RDKit (www.rdkit.org). For training purposes we normalize the properties values to a zero mean and a standard deviation of one.

Sampling from the reward-based distribution During training, we need samples from $\bar{R}(\mathbf{x}|\mathbf{y}_i)$ for each \mathbf{y}_i from the training set. We define the reward as

$$R(\mathbf{x}; \mathbf{y}_i) = \begin{cases} \exp(-\lambda \ell_1(f(\mathbf{x}), \mathbf{y}_i)), & \text{if } \ell_1(f(\mathbf{x}), \mathbf{y}_i) \leq \epsilon \\ 0, & \text{otherwise,} \end{cases} \quad (12)$$

where $\ell_1(\cdot, \cdot)$ is the ℓ_1 distance of its arguments, and λ is a temperature hyper-parameter that prevents $p(\cdot|i)$, i.e., the approximation of $\bar{R}(\mathbf{x}; \mathbf{y}_i)$ using the training set, from becoming uniform over the non-zero reward samples; it controls how peaked is the $p(\cdot|i)$ distribution at the ground truth. We determine the values of the hyper-parameters based on the statistics of the $\ell_1(f(\mathbf{x}_j), \mathbf{y}_i)$ distance on the training set, details are explained section D. We pre-compute the probability table $p(\cdot|i)$ for all \mathbf{y}_i in the training set and save the non-zero entries and the corresponding \mathbf{x} indices. During training, for each \mathbf{y}_i in the mini batch, we sample ten \mathbf{x} samples from $p(\cdot|i)$.

Results To evaluate the performance we do one sample generation for each \mathbf{y}_i in the test set from the learned model $p_\theta(\mathbf{x}|\mathbf{y}_i)$. In Table 3, we provide the generation performance results over full test set. In the Table 5, we present the result for conditional generation where we do one sample generation per \mathbf{y}_i and calculate the error between the obtained molecules property and target \mathbf{y}_i . To account for the randomness that occur due to the sampling, we repeat such process ten times and report the statistics over ten trials. In the case of ChEMBL, repeating such generation ten times over a test set of size 238k was too expensive so we limited to 10k randomly selected instances. In Appendix G we report the results of a single molecule sampling over the full test set, consistent with the results we provide here.

For QM9 our model has smaller MSE than the ML baseline model and better correlation on all properties. In the larger ChEMBL dataset the results are mixed, with our model achieving an MSE lower than that of the ML in five out of the nine properties and higher in the remaining four. More results are presented included in appendix (Table G.1).

To check the plausibility of the generated molecules, we then run a series of quality filters from Brown et al. [5], which aim to detect those which are “*potentially unstable, reactive, laborious to synthesize, or simply unpleasant*”. Of our valid generated molecules, we find 71.3% pass the quality filters, nearly the same success rate as the test set molecules themselves, 72.2%; if we were to normalize as in Table 1 of Bradshaw et al. [4], our performance of $\approx 98.7\%$ outperforms nearly all approaches considered. Figure 1 shows example generations from the model trained on the ChEMBL, 12 out of

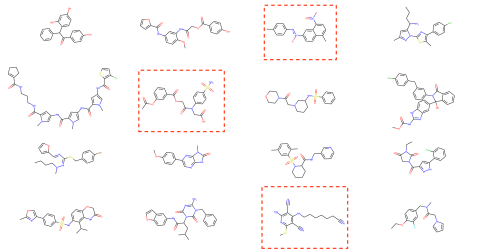


Figure 1: Example generated molecules from the ChEMBL model; red indicates failing the quality filters.

Target	Kang & Cho	Ours
MolWt=250	250.3±6.7	253.8 ±11.8
MolWt = 350	349.6±7.3	351.7 ±12.5
MolWt = 450	449.6±8.9	450.9±13.2
Logp = 1.5	1.539±0.301	1.571±0.371
Logp = 3	2.984±0.295	3.034± 0.348
Logp = 4.5	4.350±0.309	4.499±0.338
QED= 0.5	0.527±0.094	0.502±0.079
QED = 0.7	0.719±0.088	0.691 ±0.063
QED = 0.9	0.840± 0.070	0.882± 0.044

Table 6: Comparing with the conditional VAE model of Kang and Cho [14] on the conditional molecule generation task.

16 generated molecules passed the quality filter. In Fig. K.9 in appendix we provide an example of ten generations our QM9 model produces when we condition on a given target property vector. Among the ten generated molecules we have nine distinct ones. Five of these (the boxed ones) have never been seen in the training set. QM9 does not represent any real molecule distribution — we do note that all the molecules we show have 9 heavy atoms, consistent with the training dataset. Our model does not simply rank and propose training instances for a given property: it successfully generates novel molecules.

3.3 Testing against a strong baseline: Data augmentation -based sampling

Here we explore two additional data augmentation -based approaches to sampling of learning instances for the molecule generation datasets. The first of these is RAML [18], which maximizes a conditional log probability of the augmented versions of the training instances. Given a training instance $(\mathbf{x}^*, \mathbf{y}^*)$, it samples from a distribution $q(\mathbf{x}|\mathbf{x}^*; \tau)$ which is implicitly defined by an appropriate augmentation/perturbation strategy from the training instance \mathbf{x}^* . It was designed for text tasks such as machine translation, where for example the training instances correspond to sentences in a source and target language. In that setting an effective perturbation strategy is simply an edit-distance-based modification of the \mathbf{x}^* instance. Such an approach will work well when the augmentation strategy produces instances $\mathbf{x} \sim q(\mathbf{x}|\mathbf{x}^*; \tau)$ which will exhibit a property \mathbf{y} that does not significantly stray away from \mathbf{y}^* — that is, $f(\mathbf{x}) \approx f(\mathbf{x}^*)$ when \mathbf{x} and \mathbf{x}^* are close in edit distance. We will evaluate the ability of edit-distance-based augmentation to generate sequences whose properties are close to those of the original training sequence \mathbf{x}^* , with edit-distance-based RAML as a baseline. In addition, since we can evaluate the properties of the augmented sequences we will do so and add the resulting $(\mathbf{x}, \mathbf{y} = f(\mathbf{x}))$ instances in the an extended training set, in what can be seen as a standard data augmentation strategy for an additional baseline. Note this is only possible because in this particular setting we are able to evaluate our ground truth function f ; in general one cannot expect this to be available.

We also tested a REINFORCE approach where we actually use a score function gradient estimator (Eq. 2), with warm-start from a model trained with maximum likelihood. This is uncompetitive with any of the other baselines; we discuss these RL results in Appendix I, and Tables I.4 and I.5. Moreover, we also compare with other existing models that purely designed for conditional molecule generation. Most other work for molecule generation cannot do so in one step, instead using the model as part of an iterative optimization procedure (e.g. RL or Bayesian optimization). The most competitive model we are aware of is Kang and Cho [14], which can indeed do direct conditional generation. In Table 6 we compare our results using the ChEMBL-trained model on the task considered in their paper, generating conditioned on a single target property. Despite our model not being tailored for this task, we perform similarly well or better in terms of property accuracy, and furthermore, we do so *far faster* — their model employs a beam search decoder averaging 4.5 *seconds* per molecule, with ours requiring 6 *milliseconds*.

Edit distance on SMILES We first study the appropriateness of the edit-distance-based augmentations, used in RAML, in the sequence problems we examine. Given a sampled SMILES string from the training set we do m edit-distance-based perturbations of it by removing, inserting or swapping m number of the characters. We sample randomly 100 SMILES string from the training set and

m	validity	unicity	MSE
One	0.265	0.322	194.945
Two	0.095s	0.421	468.556
Three	0.046	0.393	725.128
Four	0.0276	0.422	985.451
Five	0.0204	0.480	1496.023
Six	0	-	-

Table 7: Edit distance augmentation evaluation on QM9 dataset

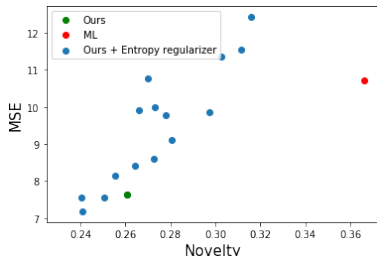


Figure 2: Effect of the entropy on the generated sequences from the validation set.

Model	# rotatable bonds	# aromatic ring	QM9: MSE						
			logP	QED	TPSA	bertz	molecule weight	fluorine count	# rings
Classic data augmentation	0.0584	0.0107	0.0631	0.0017	7.7358	133.6868	6.4299	0.0009	0.0755
RAML-like data augmentation	0.9666	0.0876	0.5991	0.0071	181.7502	2677.7330	2031.7948	0.0182	0.5356
Ours + entropy ($\lambda = 0.0008$)	0.0228	0.0007	0.0262	0.0007	6.3374	80.2370	2.2935	0.0006	0.0191
QM9: Correlation coefficient									
Classic data augmentation	0.976660	0.970758	0.969238	0.853202	0.991058	0.969615	0.914065	0.987762	0.971779
RAML-like data augmentation	0.662532	0.665283	0.724079	0.499901	0.790727	0.554120	0.080851	0.795729	0.817079
Ours + entropy ($\lambda = 0.0008$)	0.990437	0.999046	0.987524	0.941259	0.992992	0.983400	0.982855	0.980721	0.994428

Table 8: Conditional generation performance for the molecule datasets of the data augmentation based sampling and our entropy regulariser. Due to space constraints, standard deviations are omitted here, but can be found in Appendix Table L.7.

generate for each one of them 1000 augmentations for every $m \in [1, 6]$. We report the validity and uniqueness of the perturbed molecules and the distance (MSE) of their properties from the properties of the original molecule in Table 7.

As we can see in Table 7, the property of a molecule is very sensitive to perturbations. The same holds for the integer expressions as well. Even a one character edit can lead to a drastic property change. This puts into question the use of edit-distance-based augmentations as a means to sample learning instances when we deal with sequences that are sensitive to local perturbations.

Importance sampling with edit distance proposals Although our approach restricts the domain of the normalized rewards distribution to allow easy sampling, our reward function Eq. (12) is able to assign reward for any given sequence. Since the edit-distance-based augmentation can propose new sequences, we can use the $q(\mathbf{x}|\mathbf{x}^*, \tau)$ as a proposal distribution and importance sample, with

$$\mathbb{E}_{\bar{R}(\mathbf{x}|\mathbf{y}^*)} [\log p_{\theta}(\mathbf{x}|\mathbf{y}^*)] = \mathbb{E}_{q(\mathbf{x}|\mathbf{x}^*, \tau)} \left[\frac{\bar{R}(\mathbf{x}|\mathbf{y}^*)}{q(\mathbf{x}|\mathbf{x}^*, \tau)} \log p_{\theta}(\mathbf{x}|\mathbf{y}^*) \right].$$

We follow the same edit distance sampling process as Norouzi et al. [18] and set $\tau = 0.745$ so that if we sample 10 values, the zero edit distance will be sampled with $p = 0.1$. The average ℓ_1 distance of the properties of the augmented instances from the target property is 4641.0. As a result most of the sequences proposed by $q(\mathbf{x}|\mathbf{x}^*, \tau)$ will have $\bar{R}(\mathbf{x}|\mathbf{y}^*) = 0$ and contribute nothing to learning.

Data augmentation on SMILES Even though the edit distance does not preserve properties, we can still evaluate their properties using RDKit; thus, we can pair every augmented instance \mathbf{x} with its evaluated property $f(\mathbf{x})$, and add these couples in the training dataset. We call this baseline ‘‘Classic data augmentation’’. For completeness we will also evaluate the ‘‘RAML-like data augmentation’’ where we pair the augmented instances \mathbf{x} with the property of the original \mathbf{x}^* from which they were produced, even though as we have seen such a pairing is not appropriate.

In Table 4 we give the quality of the generations of the augmentation-based sampling approaches. In terms of validity the two augmentation-based approaches have a lower performance compared to our method in Table 3. For novelty they have considerably higher scores, to be expected since they are actually generating new training data. However, when it comes to the quality of the conditional generations, as measured by MSE in, Table 8, as expected the RAML-based approach performs very poorly, and while ‘‘Classic data augmentation’’ performs acceptably is it still considerably worse than our training method results in Table 5.

3.4 Deploying the entropy-based regulariser

Our basic approach achieves a high novelty score on the larger ChEMBL dataset. However this is not the case for the smaller dataset QM9. In an effort to improve the novelty of our method in small data regimes, we introduce the entropy regulariser, from Eq. (10). We evaluate its effect for λ in a range of values from 0.0001 to 0.005 for QM9, using the same experimental settings as above. We measured trained models’ generation performance on the hold out validation set. Uniqueness stays rather stable, while validity slightly drops as λ increases. Fig. 2 shows there is a trade-off between novelty and conditional generation performance: increased novelty comes at the cost of property MSE. In Tables 4 and 8, we include the results of using the entropy-regularized model trained with a λ value that improves the novelty while still matching MSE performance of ML training.

4 Related work

Neural sequence models [2, 23] are typically trained via maximum likelihood estimation. However, the log-likelihood objective is only measured on the ground truth input-output pairs: such training does not take into account the fact that for a target property, there exist many candidates that are different from the ground truth but still acceptable. To account for such a disadvantage, Norouzi et al. [18] proposed reward-augmented maximum likelihood (RAML) which adds reward-aware perturbations to the target, and Xie et al. [27] applied data noising in language models. Although these works show improvement over pure ML training, they make an implicit assumption that the underlying sequences’ properties are relatively stable with respect to small perturbations. This restricts the applicability of such models on other types of sequences than text.

An alternative is a two-stage optimization approach, in which an initial general-purpose model is later fine-tuned for conditional generation tasks. Segler et al. [22] propose using an unconditional RNN model to generate a large body of candidate sequences; goal-directed generation is then achieved by either filtering the generated candidates or fine-tuning the network. Alternatively, autoencoder-based methods map from the discrete sequence data into a continuous space. Conditioning is then done via optimization in the learned continuous latent representation [9, 15, 7], or through direct generation with a semi-supervised VAE [14] or through mutual information regularization [1]. Similar work appeared in conditional text generation [12], where a constraint is added so that the generated text matches a target property by jointly training a VAE with a discriminator.

Instead of using conditional log-likelihood as a surrogate, direct optimization of task reward has been considered a gold standard for goal-oriented sequence generation tasks. Various RL approaches have been applied for sequence generation, such as policy gradient [20] and actor-critic [3]. However, maximizing the expected reward is costly. To overcome such disadvantages, one need to apply various variance reduction techniques [10], warm starting from a pre-trained model, incorporating beam search [26, 6] or a replay buffer during training. More recent works also focused on replacing the sampling distribution with some other complicated distribution which takes into account both the model and reward distribution [8]. However, those techniques are still expensive and hard to train. Our work in this paper aims to develop an easy alternative to optimize the expected reward.

5 Conclusion

We present a simple, tractable, and efficient approach to expected reward maximization for goal-oriented discrete structure generation tasks. By sampling directly from the approximate normalized reward distribution, our model eliminates the sample inefficiency faced when using a score function gradient estimator to maximize the expected reward. We present results on two conditional generation tasks, finding significant reductions in conditional generation error across a range of baselines.

One potential concern with this approach would be that reliance on a training dataset could reduce novelty of generations, relative to reinforcement learning algorithms that actively propose new structures during training. This is particularly a concern in a low-data regime: while the entropy-based regularization can help, it may not be enough to help discover (say) entire modes missing from the training dataset. We leave this exploration to future work. However, in some settings the implicit bias of the dataset may be beneficial: if the training data all is drawn from a distribution of “plausible” values, then deviations too far from training examples may be undesirable. For example, in some molecule design settings the reward may be measured by a machine learning property predictor, fit to its own training dataset; if an RL algorithm finds points the property predictor suggests are promising, but are far from the training data, they may be spurious false positives.

Broader Impact

When a training dataset of suitable examples is available, the methodology introduced by this paper provides an easy approach to learning conditional models. These models otherwise would be fit using an expensive reinforcement learning algorithm, or by less-performant maximum likelihood estimation. Our hope is that learning algorithms that are simpler to tune can help drive adoption of machine learning methods by the broader scientific community, and may help reduce computational and energy requirements for training these models. Furthermore, we are not aware of existing work that trains a single model capable of conditional generation of molecules given such a diverse set of properties; we believe this application and its results will be of independent interest to the computational chemistry community.

Acknowledgments and Disclosure of Funding

This work was supported by the Alan Turing Institute under the EPSRC grant EP/N510129/1 and the RCSO ISNet within the "Machine learning tools for target molecule design" project.

References

- [1] R. Assouel, M. Ahmed, M. H. Segler, A. Saffari, and Y. Bengio. Defactor: Differentiable edge factorization-based probabilistic graph generation. *CoRR*, abs/1811.09766, 2018. URL <http://arxiv.org/abs/1811.09766>.
- [2] D. Bahdanau, K. Cho, and Y. Bengio. Neural machine translation by jointly learning to align and translate. *arXiv preprint arXiv:1409.0473*, 2014.
- [3] D. Bahdanau, P. Brakel, K. Xu, A. Goyal, R. Lowe, J. Pineau, A. Courville, and Y. Bengio. An actor-critic algorithm for sequence prediction. *arXiv preprint arXiv:1607.07086*, 2016.
- [4] J. Bradshaw, B. Paige, M. J. Kusner, M. Segler, and J. M. Hernández-Lobato. A model to search for synthesizable molecules. In *Advances in Neural Information Processing Systems 32*, pages 7935–7947. 2019.
- [5] N. Brown, M. Fiscato, M. H. Segler, and A. C. Vaucher. Guacamol: benchmarking models for de novo molecular design. *Journal of chemical information and modeling*, 59(3):1096–1108, 2019.
- [6] R. Bunel, M. Hausknecht, J. Devlin, R. Singh, and P. Kohli. Leveraging grammar and reinforcement learning for neural program synthesis. *arXiv preprint arXiv:1805.04276*, 2018.
- [7] H. Dai, Y. Tian, B. Dai, S. Skiena, and L. Song. Syntax-directed variational autoencoder for structured data. *arXiv preprint arXiv:1802.08786*, 2018.
- [8] N. Ding and R. Soricut. Cold-start reinforcement learning with softmax policy gradient. In *Advances in Neural Information Processing Systems*, pages 2817–2826, 2017.
- [9] R. Gómez-Bombarelli, D. K. Duvenaud, J. M. Hernández-Lobato, J. Aguilera-Iparraguirre, T. D. Hirzel, R. P. Adams, and A. Aspuru-Guzik. Automatic chemical design using a data-driven continuous representation of molecules. *CoRR*, abs/1610.02415, 2016. URL <http://arxiv.org/abs/1610.02415>.
- [10] E. Greensmith, P. L. Bartlett, and J. Baxter. Variance reduction techniques for gradient estimates in reinforcement learning. *Journal of Machine Learning Research*, 5(Nov):1471–1530, 2004.
- [11] G. L. Guimaraes, B. Sanchez-Lengeling, C. Outeiral, P. L. C. Farias, and A. Aspuru-Guzik. Objective-reinforced generative adversarial networks (organ) for sequence generation models. *arXiv preprint arXiv:1705.10843*, 2017.
- [12] Z. Hu, Z. Yang, X. Liang, R. Salakhutdinov, and E. P. Xing. Toward controlled generation of text. In *Proceedings of the 34th International Conference on Machine Learning-Volume 70*, pages 1587–1596. JMLR. org, 2017.
- [13] F. Huszár. How (not) to train your generative model: Scheduled sampling, likelihood, adversary? *arXiv preprint arXiv:1511.05101*, 2015.

- [14] S. Kang and K. Cho. Conditional molecular design with deep generative models. *Journal of chemical information and modeling*, 59(1):43–52, 2018.
- [15] M. J. Kusner, B. Paige, and J. M. Hernández-Lobato. Grammar variational autoencoder. *arXiv preprint arXiv:1703.01925*, 2017.
- [16] S. Lacoste-Julien, F. Huszár, and Z. Ghahramani. Approximate inference for the loss-calibrated bayesian. In *Proceedings of the Fourteenth International Conference on Artificial Intelligence and Statistics*, pages 416–424, 2011.
- [17] D. Mendez, A. Gaulton, A. P. Bento, J. Chambers, M. De Veij, E. Félix, M. P. Magariños, J. F. Mosquera, P. Mutowo, M. Nowotka, et al. ChEMBL: towards direct deposition of bioassay data. *Nucleic acids research*, 47(D1):D930–D940, 2018.
- [18] M. Norouzi, S. Bengio, N. Jaitly, M. Schuster, Y. Wu, D. Schuurmans, et al. Reward augmented maximum likelihood for neural structured prediction. In *Advances In Neural Information Processing Systems*, pages 1723–1731, 2016.
- [19] R. Ramakrishnan, P. O. Dral, M. Rupp, and O. A. Von Lilienfeld. Quantum chemistry structures and properties of 134 kilo molecules. *Scientific data*, 1:140022, 2014.
- [20] M. Ranzato, S. Chopra, M. Auli, and W. Zaremba. Sequence level training with recurrent neural networks. *arXiv preprint arXiv:1511.06732*, 2015.
- [21] J. Schulman, N. Heess, T. Weber, and P. Abbeel. Gradient estimation using stochastic computation graphs. In *Advances in Neural Information Processing Systems*, pages 3528–3536, 2015.
- [22] M. H. Segler, T. Kogej, C. Tyrchan, and M. P. Waller. Generating focused molecule libraries for drug discovery with recurrent neural networks. *ACS central science*, 4(1):120–131, 2017.
- [23] I. Sutskever, O. Vinyals, and Q. V. Le. Sequence to sequence learning with neural networks. In *Advances in neural information processing systems*, pages 3104–3112, 2014.
- [24] D. Weininger. Smiles, a chemical language and information system. 1. introduction to methodology and encoding rules. *Journal of chemical information and computer sciences*, 28(1):31–36, 1988.
- [25] R. J. Williams. Simple statistical gradient-following algorithms for connectionist reinforcement learning. *Machine learning*, 8(3-4):229–256, 1992.
- [26] S. Wiseman and A. M. Rush. Sequence-to-sequence learning as beam-search optimization. *arXiv preprint arXiv:1606.02960*, 2016.
- [27] Z. Xie, S. I. Wang, J. Li, D. Lévy, A. Nie, D. Jurafsky, and A. Y. Ng. Data noising as smoothing in neural network language models. *arXiv preprint arXiv:1703.02573*, 2017.

A Equivalent formulation of the expected reward

$$\begin{aligned}
\mathbb{E}_{p_\theta(\mathbf{x}|\mathbf{y})}[R(\mathbf{x}; \mathbf{y})] &= \sum_{\mathbf{x}} [p_\theta(\mathbf{x}|\mathbf{y})R(\mathbf{x}; \mathbf{y})] \\
&= \sum_{\mathbf{x}} \left[\frac{R(\mathbf{x}; \mathbf{y})}{\sum_{\mathbf{x}} R(\mathbf{x}; \mathbf{y})} p_\theta(\mathbf{x}|\mathbf{y}) (\sum_{\mathbf{x}} R(\mathbf{x}; \mathbf{y})) \right] \\
&= (\sum_{\mathbf{x}} R(\mathbf{x}; \mathbf{y})) \sum_{\mathbf{x}} \left[\frac{R(\mathbf{x}; \mathbf{y})}{\sum_{\mathbf{x}} R(\mathbf{x}; \mathbf{y})} p_\theta(\mathbf{x}|\mathbf{y}) \right] \\
&= c(\mathbf{y}) \sum_{\mathbf{x}} [\bar{R}(\mathbf{x}|\mathbf{y}) p_\theta(\mathbf{x}|\mathbf{y})] \\
&= c(\mathbf{y}) \mathbb{E}_{\bar{R}(\mathbf{x}|\mathbf{y})} p_\theta(\mathbf{x}|\mathbf{y})
\end{aligned} \tag{13}$$

where $c(\mathbf{y}) = \sum_{\mathbf{x}} R(\mathbf{x}; \mathbf{y})$, $\bar{R}(\mathbf{x}|\mathbf{y}) = R(\mathbf{x}; \mathbf{y})/c(\mathbf{y})$

B Approximating the normalized reward

As our final objective presented in Equation (5), we need to draw samples from the normalized reward distribution $\bar{R}(\mathbf{x}|\mathbf{y}_i)$. We proposed an distribution $p(i, j)$ which is defined on training data to approximate such distribution. Here we are going to discuss the derivation of such approximation and it's effect on the final learning.

$$\begin{aligned}
\mathbb{E}_{\bar{R}(\mathbf{x}|\mathbf{y}_i)}[\log p_\theta(\mathbf{x}|\mathbf{y}_i)] &\approx \sum_{j=1}^N [\bar{R}(\mathbf{x}_j|\mathbf{y}_i) \log p_\theta(\mathbf{x}_j|\mathbf{y}_i)] \\
&= \sum_{j=1}^N \left[\frac{R(\mathbf{x}_j; \mathbf{y}_i)}{\sum_{\mathbf{x}} R(\mathbf{x}; \mathbf{y}_i)} \log p_\theta(\mathbf{x}_j|\mathbf{y}_i) \right] \\
&= \sum_{j=1}^N \left[\frac{R(\mathbf{x}_j; \mathbf{y}_i)}{\sum_{\mathbf{x}} R(\mathbf{x}; \mathbf{y}_i)} \frac{\sum_{j=1}^N R(\mathbf{x}_j; \mathbf{y}_i)}{\sum_{j=1}^N R(\mathbf{x}_j; \mathbf{y}_i)} \log p_\theta(\mathbf{x}_j|\mathbf{y}_i) \right] \\
&= \sum_{j=1}^N \left[\frac{\sum_{j=1}^N R(\mathbf{x}_j; \mathbf{y}_i)}{\sum_{\mathbf{x}} R(\mathbf{x}; \mathbf{y}_i)} \frac{R(\mathbf{x}_j; \mathbf{y}_i)}{\sum_{j=1}^N R(\mathbf{x}_j; \mathbf{y}_i)} \log p_\theta(\mathbf{x}_j|\mathbf{y}_i) \right] \\
&= \frac{\sum_{j=1}^N R(\mathbf{x}_j; \mathbf{y}_i)}{\sum_{\mathbf{x}} R(\mathbf{x}; \mathbf{y}_i)} \sum_{j=1}^N \left[\frac{R(\mathbf{x}_j; \mathbf{y}_i)}{\sum_{j=1}^N R(\mathbf{x}_j; \mathbf{y}_i)} \log p_\theta(\mathbf{x}_j|\mathbf{y}_i) \right] \\
&= \frac{\sum_{j=1}^N R(\mathbf{x}_j; \mathbf{y}_i)}{\sum_{\mathbf{x}} R(\mathbf{x}; \mathbf{y}_i)} \mathbb{E}_{p(j|i)}[\log p_\theta(\mathbf{x}_j|\mathbf{y}_i)] \\
&\approx \mathbb{E}_{p(j|i)}[\log p_\theta(\mathbf{x}_j|\mathbf{y}_i)]
\end{aligned} \tag{14}$$

where $p(j|i)$ is defined as

$$p(j|i) = \frac{R(\mathbf{x}_j; \mathbf{y}_i)}{\sum_{j=1}^N R(\mathbf{x}_j; \mathbf{y}_i)}. \tag{15}$$

$$\bar{R}(\mathbf{x}|\mathbf{y}_i) = \frac{R(\mathbf{x}; \mathbf{y}_i)}{\sum_{\mathbf{x}} R(\mathbf{x}; \mathbf{y}_i)} \tag{16}$$

Note that the original normalized distribution $\bar{R}(\mathbf{x}|\mathbf{y}_i)$ is defined on all possible \mathbf{x} and normalized by $\sum_{\mathbf{x}} R(\mathbf{x}; \mathbf{y}_i)$, which is the summation over all possible \mathbf{x} , while the distribution $p(i, j)$ is defined only on the training set and therefore normalized by $\sum_{j=1}^N R(\mathbf{x}_j; \mathbf{y}_i)$ which is summation over all \mathbf{x} that are in the training set. The last approximation in equation 14 is off by a scalar multiplication factor $\sum_{j=1}^N R(\mathbf{x}_j; \mathbf{y}_i) / \sum_{\mathbf{x}} R(\mathbf{x}; \mathbf{y}_i)$.

However, this factor does not dramatically affect outcomes for two reasons. First, its value *independent of the value of \mathbf{x}* , depending only on \mathbf{y}_i . Any bias which is introduced would come into play only in the evaluation of equation 6, where entries from different \mathbf{y} values may effectively be assigned different weights. So while this may affect unconditional generations from the model, and means that some \mathbf{y} values may be considered “more important” during training, it should not directly bias *conditional* generation for a fixed \mathbf{y} .

Second, this can be thought of as a ratio of two expectations; the numerator w.r.t. a uniform distribution on \mathbf{x} and the denominator w.r.t. the empirical data distribution $\tilde{p}(\mathbf{x})$. For one of the empirical examples (on QM9), this ratio has an expected value of 1.0, since the dataset itself is constructed by enumeration of all molecules with up to 9 heavy atoms and thus also follows a uniform distribution over the domain.

For the other examples, if the training data well represents the underlying conditional distribution, that scaling factor should be almost equal for all \mathbf{y} in the training set and dropping this term would not affect the optimization. This is because both terms correspond to estimates of expected reward — they only differ if values of \mathbf{x} which have high probability under the uniform distribution (and low probability under the data distribution) also *have high reward for a given target \mathbf{y}_i* . This factor then should not vary largely unless significant modes of \mathbf{x} are missing from the training data for some values of \mathbf{y}_i , but not for others.

C Gradient of the entropy

The gradient of the exact entropy term can be calculated as following using log derivative trick:

$$\begin{aligned}
 \nabla_{\theta} H(p_{\theta}(\mathbf{x}|\mathbf{y})) &= -\nabla_{\theta} \left[\sum_{\mathbf{x}} p_{\theta}(\mathbf{x}|\mathbf{y}) \log p_{\theta}(\mathbf{x}|\mathbf{y}) \right] & (17) \\
 &= -\sum_{\mathbf{x}} \nabla_{\theta} [p_{\theta}(\mathbf{x}|\mathbf{y}) \log p_{\theta}(\mathbf{x}|\mathbf{y})] \\
 &= -\sum_{\mathbf{x}} [p_{\theta}(\mathbf{x}|\mathbf{y}) \nabla \log p_{\theta}(\mathbf{x}|\mathbf{y}) + \log p_{\theta}(\mathbf{x}|\mathbf{y}) \nabla_{\theta} p_{\theta}(\mathbf{x}|\mathbf{y})] \\
 &= -\sum_{\mathbf{x}} (1 + \log p_{\theta}(\mathbf{x}|\mathbf{y})) p_{\theta}(\mathbf{x}|\mathbf{y}) \nabla_{\theta} \log p_{\theta}(\mathbf{x}|\mathbf{y}) \\
 &= -\mathbb{E}_{p_{\theta}(\mathbf{x}|\mathbf{y})} [(1 + \log p_{\theta}(\mathbf{x}|\mathbf{y})) \nabla_{\theta} \log p_{\theta}(\mathbf{x}|\mathbf{y})]
 \end{aligned}$$

D Description of the model structure and experiments setup

Model structure To model the conditional distribution $p_{\theta}(\mathbf{x}|\mathbf{y})$, we modified the Segler et al. [22], Brown et al. [5] sequence model which was initially designed to learn $p_{\theta}(\mathbf{x})$. The pipeline of the model is presented in figure D.3. We set a maximum length of the sequence $T = 100$. By adding a start and stop token, we represent each sequence with a $T + 2$ length vector, each element of which is an index in the dictionary. We use zero padding whenever it is necessary. Each element of the $T + 2$ vector is embedded to a h -dimensional vector ($h=512$) through an embedding layer and concatenate with its c -dimensional property vector. Thus each sequence/molecule is represented with a $(T + 2) \times (h + c)$ matrix. We feed this matrix to an LSTM with three hidden layers with hidden state dimension 512. The output of LSTM last hidden layers is then feed to a linear layer to generates the resulting sequence which is given by a $(T + 2) \times D$ matrix where D refers to the dictionary size that used to describe the sequences.

experimental setups We set the batch size to 20, maximum epoch number to 100 and learning rate of the Adam optimizer to 0.001. We early stop when the validation set performance decreases by a factor of two over the best validation performance obtained so far. Since our learning task is generating sequences that exhibit a given set of desired properties, \mathbf{y} , i.e. the properties over which we do the conditioning, we define the validation set performance as the error between the set of properties \mathbf{y}' that the sequence we generate by deterministic decoding from the learned model exhibits, and the desired set properties \mathbf{y} over which we conditioned the generation.

Datasets For the QM9 dataset, we split it into a train, a validation, and a test set with 113k, 10k, an 10k instances, respectively. For the ChEMBL dataset [17], we particularly consider the subset of

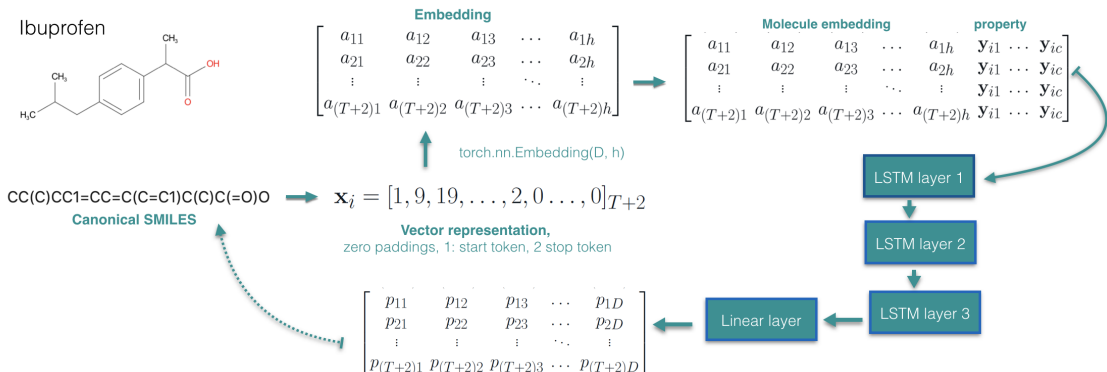


Figure D.3: Model pipeline

1600k molecules used for benchmarking by Brown et al. [5]. This dataset is divided in a training set, a validation set and a test set with roughly 1273k, 79k, and 238k instances respectively.

Hyper parameter setting The value of λ and ϵ in equation 12 are set based on the statistics of $\ell_1(f(\mathbf{x}_j), \mathbf{y}_i)$. Our goal is to have a decent number of suggested \mathbf{x} 's that have a property vector that is within ℓ_1 distance of ϵ from the desired property vector: a simple heuristic is to choose them such that, if we plan at train time to draw K samples from $p(\cdot|i)$, we see the original paired values \mathbf{x}_j with probability roughly $1/K$; appropriate values of ϵ can then be selected by inspecting the dataset. For example, when we condition on 9 properties in QM9, while sampling $K = 10$ values of \mathbf{x}_j for each \mathbf{y}_i when evaluating the loss, we set $\epsilon = 0.3$ and $\lambda = 1$: under these values for any given \mathbf{y} from the training set we have a minimum of one and a maximum of 168 suggested \mathbf{x} 's, with an average of 13. Similarly for ChEMBL dataset, we set $\epsilon = 0.4$. If we condition on a single, smooth, property, such as LogP, we set $\epsilon = 5 \times 10^{-5}$ and $\lambda = 10^5$, since in that case we can find many molecules that have a practically identical properties.

E Python expressions dataset generation

. We generate synthetic training data by sampling from the probabilistic context free grammar presented in Listing 1. We filter the generated expressions to keep only those that evaluate to a value in the range $(-1000, 1000)$, and where the overall length of the expression is at most 30 characters. We generate 500,000 samples and after removing duplicates are left with 308,722 unique (expression, value) pairs. Out of these we set aside 20k pairs as a validation set and an additional 10k as a test set. To learn the conditional generative model $p_\theta(\mathbf{x}|\mathbf{y})$, we rescale the input values \mathbf{y} by a factor of 1000, to ensure that the inputs to the LSTM are in the interval $(-1, 1)$.

F Additional details regarding the SMILES data augmentation process

The augmentation on SMILES is done as following: for each SMILES string in the training data, we use the RAML [18] defined edit distance sampling process, setting the $\tau = 0.745$, sampling an edit distance and then applying a transformation on the SMILES string. We keep sampling until we get 10 valid molecules from each SMILES string in the training set. After filtering out replicated ones, we are left with 733k instances, which is 6 times larger than the original training set size. We then pair the augmented smiles with either the properties of the original matching molecule (i.e. the property of the original SMILES), for the RAML-style importance sampling approach, or with the properties that obtained from the RDKit chemical software for the pure data augmentation approach.

G More experimental results

In Table G.1 we provide conditional generation performance of our model and ML baseline in terms of total MSE and negative log-likelihood computed over the test set.

	QM9			ChEMBL		
	total MSE	$-\log p(\mathbf{x} \mathbf{y})$		total MSE	$-\log p(\mathbf{x} \mathbf{y})$	
ML	10.7237 ± 0.4915	0.2213440		204.4400	4.2766	
Ours	7.6398	0.2891	0.2357489	302.5634 ± 5.6231	0.2569	

Table G.1: Conditional generation performance

Table G.2 presents the results on full Guacamol ChEMBL test set in terms of generation and conditional generation performance.

Model	MSE per-property									total MSE
	On larger size sequence dataset: ChEMBL									
	# rotatable bonds	# aromatic ring	logP	QED	TPSA	bertz	molecule weight	fluorine count	# rings	
ML	0.1567	0.0376	0.1448	0.0051	27.2466	1652.6992	103.3155	0.0217	0.0264	202.4087
Ours	0.1589	0.0272	0.1331	0.0046	34.9984	2534.8578	177.042	0.0072	0.0190	290.2351

Table G.2: Conditional generation performance on ChEMBL full testset

To test if the model is able to generate diverse molecules for a given target property, we sampled 10 samples for each \mathbf{y} in the testset of QM9 and measured the validity, uniqueness, and novelty of the generated molecules. The result is presented in Table G.3.

Model	MSE per-property									Validity	Uniqueness	Novelty
	On small size sequence dataset: QM9											
	# rotatable bonds	# aromatic ring	logP	QED	TPSA	bertz	molecule weight	fluorine count	# rings			
ML	0.00918	0.00065	0.010993	0.000322	2.82087	19.56099	0.78806	0.00247	0.011853	0.96420	0.558276	0.645831
Ours	0.00400	0.00023	0.00553	0.00012	1.08904	23.19567	0.36655	0.00010	0.00232	0.98781	0.512173	0.61363
Correlation coefficient												
ML	0.996233	0.998001	0.994686	0.971792	0.996827	0.995805	0.993406	0.972188	0.995973	-	-	-
Ours	0.998357	0.999288	0.997274	0.988833	0.998773	0.99503	0.996947	0.998834	0.999213	-	-	-

Table G.3: Generation and conditional generation performance of our model when we sample 10 molecules per property vector in the testset. To calculate the MSE and correlation coefficient, we use mean of the 10 sampled molecules property as \mathbf{y}' .

H KL divergence as objective

We want to recover the true underlying data distribution $\tilde{p}(\mathbf{x}|\mathbf{y})$ as accurately as possible from the training data that is observed. The KL divergence between the model $p_\theta(\mathbf{x}|\mathbf{y})$ and true data distribution $\tilde{p}(\mathbf{x}|\mathbf{y})$ is given by

$$\begin{aligned}
 D_{KL}[p_\theta(\mathbf{x}|\mathbf{y})||\tilde{p}(\mathbf{x}|\mathbf{y})] & \\
 &= \mathbb{E}_{p_\theta(\mathbf{x}|\mathbf{y})} \log p_\theta(\mathbf{x}|\mathbf{y}) - \mathbb{E}_{p_\theta(\mathbf{x}|\mathbf{y})} \log \tilde{p}(\mathbf{x}|\mathbf{y}) \\
 &= -H(p_\theta(\mathbf{x}|\mathbf{y})) - \mathbb{E}_{p_\theta(\mathbf{x}|\mathbf{y})} \log \tilde{p}(\mathbf{x}|\mathbf{y}).
 \end{aligned} \tag{18}$$

If we minimize KL divergence in this direction,

$$\begin{aligned}
 \min_{\theta} D_{KL}[p_\theta(\mathbf{x}|\mathbf{y})||\tilde{p}(\mathbf{x}|\mathbf{y})] &\approx \\
 &\max_{\theta} \mathbb{E}_{p_\theta(\mathbf{x}|\mathbf{y})} \log \tilde{p}(\mathbf{x}|\mathbf{y}) + H(p_\theta(\mathbf{x}|\mathbf{y})),
 \end{aligned} \tag{19}$$

and assume a non-parametric form approximation of the true distribution $\tilde{p}(\mathbf{x}|\mathbf{y}) \approx \frac{\exp(R(\hat{\mathbf{x}}, \mathbf{y}_i))}{\sum_{\hat{\mathbf{x}}} \exp R(\hat{\mathbf{x}}, \mathbf{y}_i)}$, where $R(\hat{\mathbf{x}}, \mathbf{y}_i)$ refers to some reward function, we get exactly the expected reward objective with maximum entropy regularizer.

If we take KL in the opposite direction

$$\begin{aligned}
 D_{KL}[\tilde{p}(\mathbf{x}|\mathbf{y})||p_\theta(\mathbf{x}|\mathbf{y})] & \\
 &= \mathbb{E}_{\tilde{p}(\mathbf{x}|\mathbf{y})} \log \tilde{p}(\mathbf{x}|\mathbf{y}) - \mathbb{E}_{\tilde{p}(\mathbf{x}|\mathbf{y})} \log p_\theta(\mathbf{x}|\mathbf{y}) \\
 &= -H(\tilde{p}(\mathbf{x}|\mathbf{y})) - \mathbb{E}_{\tilde{p}(\mathbf{x}|\mathbf{y})} \log p_\theta(\mathbf{x}|\mathbf{y})
 \end{aligned} \tag{20}$$

we have

$$\min D_{KL}[\tilde{p}(\mathbf{x}|\mathbf{y})||p_{\theta}(\mathbf{x}|\mathbf{y})] \approx \max_{\theta} \mathbb{E}_{\tilde{p}(\mathbf{x}|\mathbf{y})} \log p_{\theta}(\mathbf{x}|\mathbf{y}). \quad (21)$$

As the expectation is taken over the true data distribution, one can empirically evaluate it on the training data pairs. This is equivalent of assuming that $\tilde{p}(\mathbf{x}|\mathbf{y}) \approx \delta(\mathbf{x}|\mathbf{y})$ and doing maximum log likelihood training on the training set. Even though both KL have a hypothetical minimum at $p_{\theta}(\mathbf{x}|\mathbf{y}) = \tilde{p}(\mathbf{x}|\mathbf{y})$, they do not achieve the same solution unless the model has enough learning capability. $D_{KL}[p_{\theta}(\mathbf{x}|\mathbf{y})||\tilde{p}(\mathbf{x}|\mathbf{y})]$ encourages $p_{\theta}(\mathbf{x}|\mathbf{y})$ to put its mass mainly on the region where true data distribution $\tilde{p}(\mathbf{x}|\mathbf{y})$ has concentrated mass, while the $D_{KL}[\tilde{p}(\mathbf{x}|\mathbf{y})||p_{\theta}(\mathbf{x}|\mathbf{y})]$ pushes $p_{\theta}(\mathbf{x}|\mathbf{y})$ to learn to cover all the region that $\tilde{p}(\mathbf{x}|\mathbf{y})$ has its mass on [16, 13].

I RL baseline

Our objective is to maximize the expected reward:

$$\mathcal{J} = \mathbb{E}_{\tilde{p}(\mathbf{y})} \mathbb{E}_{p_{\theta}(\mathbf{x}|\mathbf{y})} [R(\mathbf{x}; \mathbf{y})]. \quad (22)$$

where $R(\mathbf{x}; \mathbf{y}) = \exp\{-\lambda d(f(\mathbf{x}), \mathbf{y})\}$. Using the data distribution to approximate expectations over $\tilde{p}(\mathbf{y})$, we have:

$$\mathcal{J} \approx \frac{1}{N} \sum_{i=1}^N \mathbb{E}_{p_{\theta}(\mathbf{x}|\mathbf{y}_i)} [R(\mathbf{x}; \mathbf{y}_i)]. \quad (23)$$

where \mathbf{y}_i is sampled from training data.

Note that in our case, the model $p_{\theta}(\mathbf{x}|\mathbf{y})$ defines a distribution over discrete random variables and reward depends on non-differentiable oracle function f that return feedback on the discrete sequence \mathbf{x} that is sampled from the model $p_{\theta}(\mathbf{x}|\mathbf{y})$. Therefore, we can not directly differentiate the $\hat{\mathcal{J}}$ with respect to the model parameter θ . One way to apply gradient based optimization in this case is a to use score-function estimators of the gradient:

$$\begin{aligned} \nabla_{\theta} \mathcal{J} &\approx \frac{1}{N} \sum_{i=1}^N \mathbb{E}_{p_{\theta}(\mathbf{x}|\mathbf{y}_i)} [R(\mathbf{x}; \mathbf{y}_i) \nabla_{\theta} \log p_{\theta}(\mathbf{x}|\mathbf{y}_i)] \\ &\approx \frac{1}{NM} \sum_{i=1}^N \sum_{j=1}^M [R(\mathbf{x}_j; \mathbf{y}_i) \nabla_{\theta} \log p_{\theta}(\mathbf{x}_j|\mathbf{y}_i)]. \end{aligned} \quad (24)$$

The score-function gradient estimators have high variance. Besides, in the beginning, the output of the model mostly corresponding to invalid sequences. Therefore, we use to initialize our model from a pre-trained model as a warm-start. The pre-trained model is obtained by maximizing the log-likelihood of the training data.

In the following experiment, we train the same model with the maximum log-likelihood objective for six epochs to obtain the pre-trained model for warm start. We set sample size $M = 30$, mini-batch size = 20. We set the temperature parameter $\lambda = 0.5$. At the early stage of training, since the model is not perfect, the invalid samples proposed by the model are discarded. Note that such training is very time-consuming because during training at each mini-batch, firstly, we need to sample from the model by involves unrolling the RNN which is pretty slow when we have long sequences. Secondly, for each sampled sequence, to get the property, we need to send it to some oracle function, in this case, RDKit, which is normally implemented in CPU, this requires frequent communication between CPU and GPU which greatly increases computation time.

Model	QM9			
	Validity	Unicity	Novelty	Training time per epoch (hour)
ML	0.9619	0.9667	0.3660	0.19
Ours	0.9886	0.9629	0.2605	0.56
RL+ warm start	0.4013	0.8425	0.8497	3.05

Table I.4: Molecule generation quality of the data augmentation sampling strategies and our entropy regulariser

Model	# rotatable bonds	# aromatic ring	logP	QM9: MSE						# rings
				QED	TPSA	bertz	molecule weight	fluorine count		
ML	0.0468±0.0014	0.0014±0.0003	0.0390±0.0013	0.0010±0.0000	11.1772±0.3129	80.7725±4.4282	4.4251±0.3450	0.0023±0.0012	0.0484±0.0034	
Ours	0.0166±0.0009	0.0005±0.0005	0.0184±0.0010	0.0004±0.0000	3.8585±0.1637	63.6678±2.5520	1.1835±0.1421	0.0004±0.0003	0.0120±0.0027	
RL+ warm start	0.3711±0.0149	0.0359±0.0030	0.5285±0.0141	0.0102±0.0002	206.6262±3.4869	1023.2935±24.5836	53.1911±2.2178	0.0183±0.0031	0.4260±0.0119	
				QM9: Correlation coefficient						
ML	0.980881	0.994366	0.980527	0.906267	0.987089	0.984265	0.965101	0.978346	0.981742	
Ours	0.993745	0.997184	0.990115	0.963365	0.995382	0.984006	0.988702	1.000000	0.994824	
RL+ warm start	0.851715	0.840686	0.830349	0.460100	0.904118	0.827304	0.714198	0.760453	0.899375	

Table I.5: Conditional generation performance for the molecules datasets

Note that the computational cost for sampling from RNN and frequent communication between CPU and GPU to evaluate the properties of the sampled molecules, do not allow us to use bigger sample size. With sample size 20, after relaxing the early stopping criteria, the training still exist with training loss increases more than 10 times the minimum training loss been obtained so far.

J Different ways to approximate the Entropy term

The entropy of $p_\theta(\mathbf{x}|\mathbf{y}) = \prod_{t=1}^T p_\theta(\mathbf{x}_t|\mathbf{x}_{1:t-1}, \mathbf{y})$ is given by:

$$\begin{aligned} H[p_\theta(\mathbf{x}|\mathbf{y})] &= -E_{p_\theta(\mathbf{x}|\mathbf{y})}[\log p_\theta(\mathbf{x}|\mathbf{y})] \\ &= -E_{p_\theta(\mathbf{x}_{1:T}|\mathbf{y})} \left[\sum_{t=1}^T \log p_\theta(\mathbf{x}_t|\mathbf{x}_{1:t-1}, \mathbf{y}) \right]. \end{aligned} \quad (25)$$

A naïve Monte Carlo estimation involves sampling trajectories \mathbf{x} , given \mathbf{y} , and then evaluating the log probabilities. We call this approximation *Estimator A*:

$$\hat{H}_{MC} = -\frac{1}{S} \sum_{s=1}^S \sum_{t=1}^T \log p_\theta(\mathbf{x}_t^s|\mathbf{x}_{1:t-1}^s, \mathbf{y}) \quad (26)$$

for $\mathbf{x}_t^s \sim p_\theta(\mathbf{x}|\mathbf{y})$.

The alternative way of approximating the entropy involves decomposing this into a sequence of other entropies. In this way, we have

$$H[p_\theta(\mathbf{x}|\mathbf{y})] = H[p_\theta(\mathbf{x}_1|\mathbf{y})] + \sum_{t=2}^T E_{p_\theta(\mathbf{x}_{1:t-1}|\mathbf{y})} [H[p_\theta(\mathbf{x}_t|\mathbf{x}_{1:t-1}, \mathbf{y})]] \quad (27)$$

Since the entropy for each individual \mathbf{x}_t is cheap enough to compute directly in closed form, we can do so and just use sampling in order to generate the values we condition on at each step. We call this approximation *Estimator B*:

$$H[p_\theta(\mathbf{x}_1|\mathbf{y})] + \sum_{t=2}^T E_{p_\theta(\mathbf{x}_{1:t-1}|\mathbf{y})} [H[p_\theta(\mathbf{x}_t|\mathbf{x}_{1:t-1}, \mathbf{y})]] \approx H[p_\theta(\mathbf{x}_1|\mathbf{y})] + \sum_{t=2}^T \sum_{s=1}^S \frac{1}{S} H[p_\theta(\mathbf{x}_t|\mathbf{x}_{1:t-1}^s, \mathbf{y})] \quad (28)$$

We randomly sample a \mathbf{y} from the test set and calculated the entropy of $p_\theta(\mathbf{x}|\mathbf{y})$ using above two estimators, with different sample size. We show the histogram of the resulting entropy values over 15 trials on a trained and a random model in figures J.4 and J.5 respectively. As figure J.4 and J.5 show, the estimator B is rather stable and has less variance than estimator A, as expected. Therefore, from now on, we use estimator B, which is the Monte Carlo approximation given in the equation (27), as a gold standard reference to compare other estimators against. Unfortunately, using the estimator B involves sampling from the model distribution that we want to optimize, so we still have the problems when taking the derivative. An alternative, instead of taking a Monte Carlo approximation of the expectation in front of the each entropy term in equation (27), we could do a deterministic greedy decoding by taking the max at each \mathbf{x}_t . The below figures J.6 and J.7 show how the greedy decoding variants of estimator A and B perform against estimator B with Monte Carlo sample size one and 50. For each of the Monte Carlo estimates, we plot a normal distribution showing the mean and standard deviation of the entropy values estimated from the 15 independent trials. Greedy decoding for the values we condition on seems to work reasonably well for approximating the entropy, in both a random model and a trained model setting, which means it is good-enough to use as a regularizer during early stages of training. We also tested the straight through estimator as an alternative to the

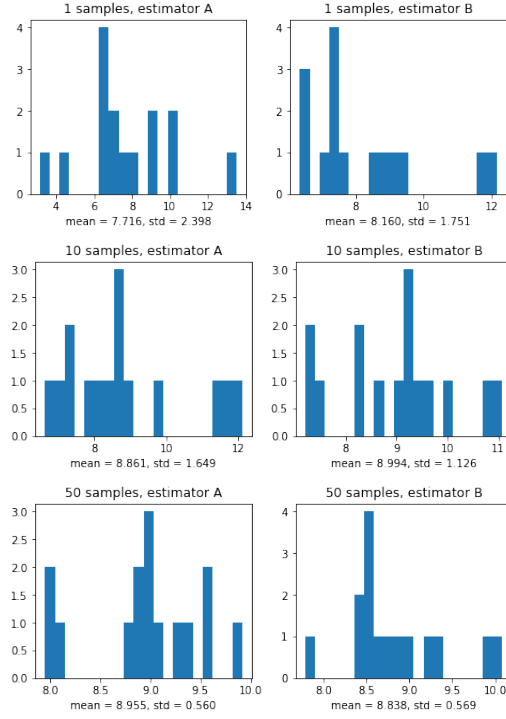


Figure J.4: The histogram of the approximated entropy of a fully-trained model $p_{\theta^*}(\mathbf{x}|\mathbf{y}_i)$

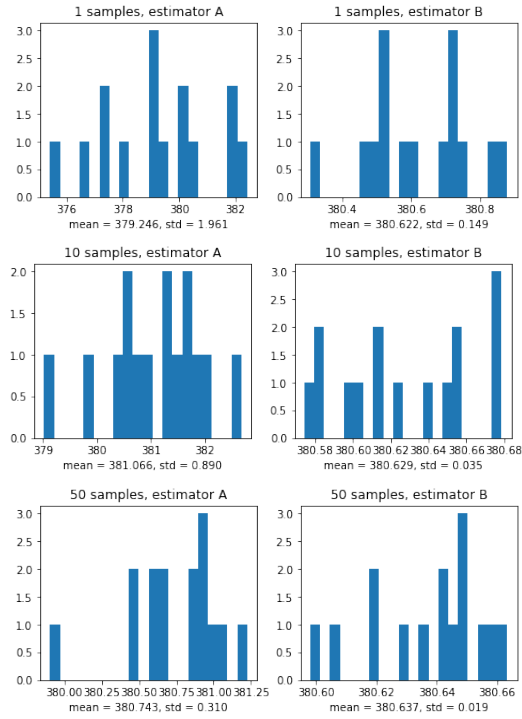


Figure J.5: The histogram of the entropy of a random model (untrained) $p_{\theta}(\mathbf{x}|\mathbf{y}_i)$

greedy decoding, as it also allows us to take gradients. To get the straight through estimator, instead

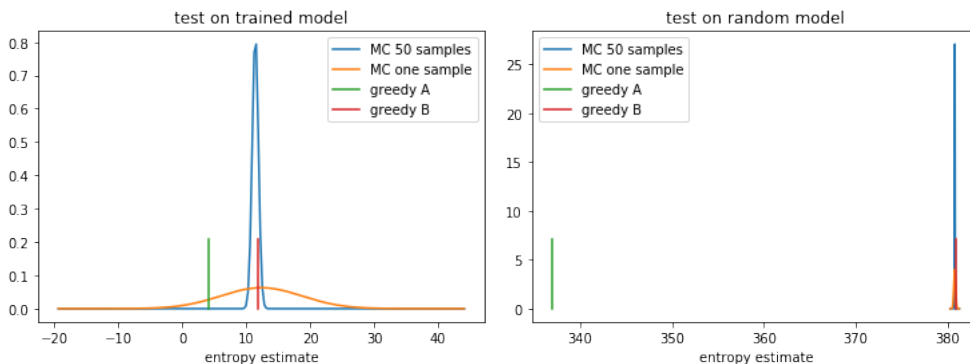


Figure J.6: Entropy approximation on the trained model

of evaluating the RNN on the embedding of a single input, we compute the mean of the embeddings under the distribution.

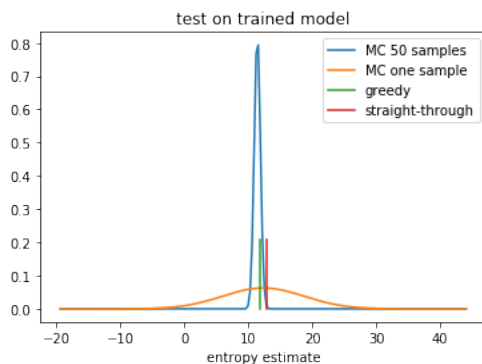


Figure J.8: Comparing a greedy and straight-through estimator to a Monte Carlo reference

The figure J.8 shows, straight through estimator also works reasonably well. In the experiment we use the greedy decoding of the estimator B,

$$\begin{aligned}
 H[p_\theta(\mathbf{x}|\mathbf{y})] &= H[p_\theta(\mathbf{x}_1|\mathbf{y})] + \\
 &\sum_{t=2}^T E_{p_\theta(\mathbf{x}_{1:t-1}|\mathbf{y})} [H[p_\theta(\mathbf{x}_t|\mathbf{x}_{1:t-1}, \mathbf{y})]] \\
 &\approx H[p_\theta(\mathbf{x}_1|\mathbf{y})] + \sum_{t=2}^T [H[p_\theta(\mathbf{x}_t|\mathbf{x}_{1:t-1}^*, \mathbf{y})]],
 \end{aligned} \tag{29}$$

where $\mathbf{x}_{1:t-1}^*$ is obtained from unrolling the RNN by taking the most probable character at each time step. For this approximation of the entropy the gradient calculation is straightforward. We can calculate the each individual entropy term analytically as our underlying sequence is discrete and finite. Therefore, the gradient calculation of this approximated entropy would be straightforward to implement and cheap in computation time.

K Molecule generation baselines

L More results

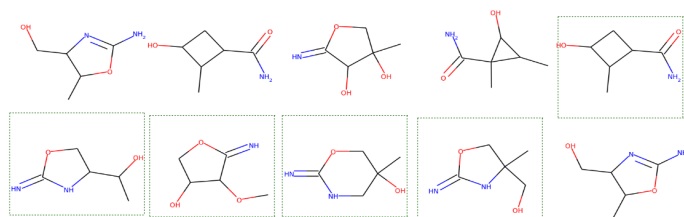


Figure K.9: Molecules generated from a given property value vector. The boxed ones are molecules that have not been seen before.

Model	# rotatable bonds	# aromatic ring	logP	QED	QM9: MSE		bertz	molecule weight	fluorine count	# rings
					TPSA	Correlation coefficient				
ML	0.0468±0.0014	0.0014±0.0003	0.0390±0.0013	0.0010±0.0000	11.1772±0.3129	80.7725±4.4282	4.4251±0.3450	0.0023±0.0012	0.0484±0.0034	
Ours	0.0166±0.0009	0.0005±0.0005	0.0184±0.0010	0.0004±0.0000	3.8585±0.1637	63.6678±2.5520	1.1835±0.1421	0.0004±0.0003	0.0120±0.0027	
ML	0.980881	0.994366	0.980527	0.906267	0.987089	0.984265	0.965101	0.978346	0.981742	
Ours	0.993745	0.997184	0.990115	0.963365	0.995382	0.984006	0.988702	1.000000	0.994824	
ChEMBL: MSE										
ML	0.1552±0.0104	0.0388±0.0028	0.1450±0.0025	0.0050±0.0001	27.6416±0.4204	1707.9996±38.8800	103.9389±3.1637	0.0128±0.0016	0.0226±0.0016	
Ours	0.1555±0.0221	0.0268±0.0018	0.1320±0.0025	0.0046±0.0001	35.0531±0.4179	2512.7421±47.7031	174.9301±3.6913	0.0074±0.0010	0.0191±0.0010	
ChEMBL: Correlation coefficient										
ML	0.993628	0.986184	0.977686	0.945018	0.990576	0.993385	0.995624	0.993952	0.993105	
Ours	0.993409	0.990111	0.979581	0.949578	0.987775	0.990189	0.992550	0.996583	0.994250	

Table L.6: Conditional generation performance for the molecules datasets

Model	QM9: MSE										
	# rotatable bonds	# aromatic ring	logP	QED	TPSA	bertz	molecule weight	fluorine count	# rings		
Classic data augmentation	0.0584	0.0107	0.0631	0.0017	7.7358	133.6868	6.4299	0.0009	0.0755		
RAML-like data augmentation	0.9666	0.0876	0.5991	0.0071	181.7502	2677.7330	2031.7948	0.0182	0.5356		
Ours + entropy ($\lambda = 0.0008$)	0.0228	0.0007	0.0262	0.0007	6.3374	80.2370	2.2935	0.0006	0.0191		
QM9: Correlation coefficient											
Classic data augmentation	0.976660	0.970758	0.969238	0.853202	0.991058	0.969615	0.914065	0.987762	0.971779		
RAML-like data augmentation	0.662532	0.665283	0.724079	0.499901	0.790727	0.554120	0.080851	0.795729	0.817079		
Ours + entropy ($\lambda = 0.0008$)	0.990437	0.999046	0.987524	0.941259	0.992992	0.983400	0.982855	0.980721	0.994428		

Table L.7: Conditional generation performance for the molecule datasets of the data augmentation based sampling and our entropy regulariser.